

## Research Article

# Cryptotanshinone Ameliorates Radiation-Induced Lung Injury in Rats

Yifang Jiang,<sup>1</sup> Fengming You,<sup>2</sup> Jie Zhu,<sup>1</sup> Chuan Zheng,<sup>3</sup> Ran Yan <sup>3</sup>, and Jinhao Zeng <sup>2</sup>

<sup>1</sup>School of Basic Medical Sciences, Chengdu University of Traditional Chinese Medicine, Chengdu 610075, China

<sup>2</sup>School of Clinical Medicine, Chengdu University of Traditional Chinese Medicine, Chengdu 610075, China

<sup>3</sup>Cancer Institute, Chengdu University of Traditional Chinese Medicine, Chengdu 610075, China

Correspondence should be addressed to Ran Yan; [yanran@cudtcm.edu.cn](mailto:yanran@cudtcm.edu.cn) and Jinhao Zeng; [zengjinhao0018@126.com](mailto:zengjinhao0018@126.com)

Received 10 July 2018; Revised 21 December 2018; Accepted 16 January 2019; Published 20 February 2019

Academic Editor: Yoshiji Ohta

Copyright © 2019 Yifang Jiang et al. This is an open access article distributed under the Creative Commons Attribution License, which permits unrestricted use, distribution, and reproduction in any medium, provided the original work is properly cited.

Cryptotanshinone (CTS) was reported to repress a variety of systemic inflammation and alleviate cardiac fibrosis, but it is still unclear whether CTS could prevent radiation-induced lung injury (RILI). Here, we investigated the effects and underlying mechanisms of CTS on a RILI rat model. Our data revealed that CTS could efficiently preserve pulmonary function in RILI rats and reduce early pulmonary inflammation infiltration elicited, along with marked decreased levels of IL-6 and IL-10. Moreover, we found that CTS is superior to prednisone in attenuating collagen deposition and pulmonary fibrosis, in parallel with a marked drop of HYP (a collagen indicator) and  $\alpha$ -SMA (a myofibroblast marker). Mechanistically, CTS inhibited profibrotic signals TGF- $\beta$ 1 and NOX-4 expressions, while enhancing the levels of antifibrotic enzyme MMP-1 in lung tissues. It is noteworthy that CTS treatment, in consistent with trichrome staining analysis, exhibited a clear advantage over PND in enhancing MMP-1 levels. However, CTS exhibited little effect on CTGF activation and on COX-2 suppression. Finally, CTS treatment significantly mitigated the radiation-induced activation of CCL3 and its receptor CCR1. In summary, CTS treatment could attenuate RILI, especially pulmonary fibrosis, in rats. The regulation on production and release of inflammatory or fibrotic factors IL-6, IL-10, TGF- $\beta$ 1, NOX-4, and MMP-1, especially MMP-1 and inhibition on CCL3/CCR1 activation, may partly attribute to its attenuating RILI effect.

## 1. Introduction

Radiation-induced lung injury (RILI) is a common and fatal complication of thoracic radiotherapy. RILI develops in almost ~5% to 20% lung cancer patients receiving radiotherapy [1] and generally leads to discontinuation of treatment. RILI is a complex pathological process mainly comprising early pneumonitis and late pulmonary fibrosis. Firstly, radiation leads to early damage of epithelial cells and inflammatory response. Next, impaired cells provoke the production and release of various inflammatory cytokines, accompanying with macrophages or neutrophils infiltration in lung tissue. In parallel, to protect against cellular injury and death, impaired cells also induce the production and release of proliferative molecules or profibrotic cytokines such as transforming growth factor- $\beta$  (TGF- $\beta$ ) [2], connective tissue growth factor (CTGF) [3], and alpha-smooth muscle actin ( $\alpha$ -SMA) [4], leading to fibroblast replication and differentiation

of fibroblast into myofibroblast. Finally, myofibroblasts produce an abundance of collagen sedimentation leading to lung fibrosis. The progressive replacement of the normal lung interstitium by fibrous tissues results in restriction of lung and gradual loss of function [5].

Macrophage inflammatory protein 1-alpha (CCL3) and its receptor CC chemokine receptor 1 (CCR1) mediate production and secretion of several key growth factors and cytokines as well as chemokine mediators [6–8], thereby playing a key role in the regulation of both inflammatory response and fibrotic process. Chemokine CCL3 dose dependently inhibited ATP-stimulated release of interleukin- (IL-) 1 $\beta$  by monocytic cells [9]. CCR1-Fc $\epsilon$ psilonRI costimulation significantly enhanced secretion of transforming growth factor beta-1, tumor necrosis factor-alpha, and the cytokine IL-6 in mast cells [7]. In return, interleukins secretion affects CCL3/CCR1-associated pathologic processes, as evidenced by a report which revealed that IL-10 neutralization in

*Streptococcus pneumoniae* infected mice was associated with augmented neutrophil recruitment and resulted in enhanced CCL3 production [10]. Also, CCR1 has been reported to regulate the recruitment of CD45(+) Collagen I (+) fibrocytes which is implicated in fibrogenic liver injury, as demonstrated by 25% inhibition of fibrocyte migration in CCR1<sup>-/-</sup> wt mice [11]. Moreover, CCL3 knockout mice displayed less inflammatory infiltrate in adenine-injured renal tissue, which also contained a striking reduction of collagen deposition and a less production of TNF- $\alpha$  [12]. The aforementioned studies revealed the contribution of CCL3/CCR1 activation in both inflammatory response and fibrotic process, and CCL3/CCR1 might serve as potential targets to ameliorate RILI. However, few studies focus on CCL3/CCR1 linking to RILI.

Currently, RILI treatment often invokes general anti-inflammatory agent corticoid clinically; various adverse effects, however, limit its application. RILI patients receiving long corticoid intervention may have varying degrees of compromised immunity, osteoporosis, peptic ulcer, hypertension, water-sodium retention, hypopotassemia, glucose-lipid metabolic disorder, etc. Hence, there is a compelling need to find novel therapies to alleviate RILI. Cryptotanshinone (CTS) is a major lipophilic extraction from *Salvia miltiorrhiza Bunge* (Danshen), an herbal dietary supplement documented in the USP 37-NF32. Also, in China, two certified compound preparations “Tanshinones capsules” (Z13020110) and “Compound Danshen dripping pills” (Z10950111), of which CTS is the major component [13, 14], were widely used more than 15 years in the market. Numerous clinical studies suggested their benefits, with no adverse events, were found, in treating acne [15], otitis externa [16], ulcerative colitis [17], hepatitis B with liver fibrosis [18], coronary heart disease [19], and hypertension [20]. Previously, CTS has been proved to be a safe extraction [14] and possess antineoplastic [21, 22], antioxidative [23], and anti-inflammatory [24, 25] bioactivities. Recently, researchers revealed that CTS was also capable of alleviating cardiac fibrosis by depressing signal transducers and activators of transcription 3 (STAT3) [26], Cyclooxygenase-2 (COX-2), NADPH oxidase-2 (NOX-2), and NOX-4 signals [27] and upregulating matrix metalloproteinase-2 (MMP-2) activation [28]. In addition, CTS was found to inhibit profibrotic activities of hypertrophic scar fibroblasts and accelerates wound healing [29]. However, the potential therapeutic effect of CTS on radiation-induced pneumonitis and fibrosis remains untested.

In this study, using a RILI rat model, we first tested whether CTS ameliorate early pneumonitis and late pulmonary fibrosis. In parallel, we observed the regulatory effects of CTS on several key inflammatory cytokines and on multiple profibrotic or antifibrotic factors. Finally, we investigated whether its potential therapeutic effect on RILI was contributed by inhibition of CCL3/CCR1 activation.

## 2. Materials and Methods

All procedures in this study were approved by the Institutional Animal Care and Use Committee (IACUC), Chengdu University of Traditional Chinese Medicine, and performed

in accordance with the approved guidelines set forth by IACUC.

**2.1. Animals.** Ninety-six male Sprague-Dawley rats (8 weeks of age, weighing 180-220g) were obtained from Chengdu Dashuo Experimental Animal Co., Ltd. (SCXK-2013-24). Animals were housed under controlled conditions of 22 $\pm$ 2°C and 60-80% relative humidity and fed with standard rodent chow and water.

**2.2. Drugs.** Cryptotanshinone (purity surpass 95%) was purchased from Xi'an He Lin Biological Engineering Co., Ltd. (110852-200806, Xi'an, China). Prednisone was obtained from Shanghai Xinyi Pharmaceutical Co., Ltd. (H31020675, Shanghai, China).

**2.3. RILI Rat Model and Treatments.** After acclimatizing with the facilities for one week, the animals were randomly assigned to the following four groups: (i) normal rats, n=24; (ii) radiation (RT) rats, n=24, the rats received lung radiation; (iii) RT+ Prednisone (PND): the rats received lung radiation plus 3.12 mg/kg PND oral administration, n=24; (iv) RT+ CTS: the rats received lung radiation plus 20 mg/kg CTS oral administration, n=24. Radiated rats were prescribed with whole lung radiation at a single dose of 14 Gy (6MV X-rays; 200kVp) after anesthetizing with intraperitoneal injection of 0.3 mL/100g chloral hydrate. During the radiation, rats were shielded with leads to protect their head, abdomen, and extremities. On the second day after radiation, treated rats were given PND or CTS by gastrogavage once a day and five days a week. Six rats in each group were sacrificed with anesthetization at months 1, 3, 5, and 8 after treatment.

**2.4. Pulmonary Function Testing.** Tidal volume, maximal voluntary ventilation, and respiratory rate were measured with an unrestrained whole body plethysmograph (Buxco, Wilmington, NC, USA) at months 1, 3, 5, and 8.

**2.5. Pulmonary Coefficient.** After sacrificing the rats, the lungs were removed, trimmed of extraneous tissue. Pulmonary coefficient was calculated by the following equation: lung wet weight (g) / body weight (kg)  $\times$  100%.

**2.6. Pathological Analysis.** Lung specimens were fixed in 10% neutral-buffered formalin overnight, embedded in paraffin, and then sliced into 5  $\mu$ m sections. The sections were stained with hematoxylin and eosin (H&E) and Masson's trichrome. The results of H&E staining were graded according to inflammatory infiltration, interstitial edema, alveolar wall integrity, and septal wall thickness. The grading was scored as follows: score 0, normal; score 1, mild (appearance of some inflammatory cells and mild focal edema, slightly widened alveolar septa); score 2, moderate (relatively apparent inflammatory infiltration, moderate edematous swelling and septal wall thickening, occasional discontinuity in the wall of alveolus); score 3, severe (numerous inflammatory cells infiltrated in alveolar septae that is severely thickened, considerable alveolar flooding, with heavy deposition of collagen, frequently

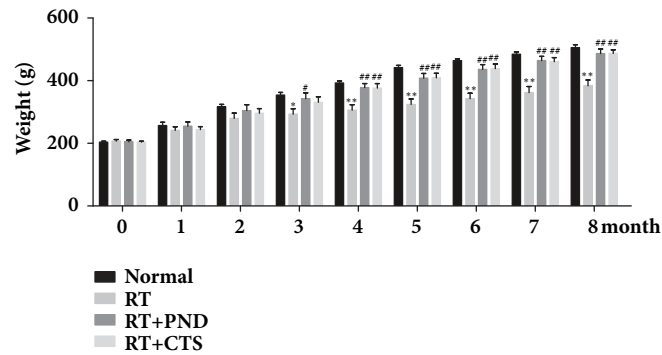


FIGURE 1: CTS prevented weight loss of RILI rats.  $n=6$ . \* $P < 0.05$  and \*\* $P < 0.01$  versus Normal; # $P < 0.05$  and ## $P < 0.01$  versus RT.

occurrence of discontinuity of alveolar wall). The Masson's trichrome staining was performed to determine the degree of interstitial fibrosis. Collagen sedimentation was assessed visually by range and distribution of blue-stained tissues. Criteria for scoring were as follows: score 0, normal; score 1, mild (slight fibrous thickening of alveolar or bronchiolar walls, without obvious lung architecture impairment); score 2, moderate (increased fibrosis with definite damage to lung architecture, and formation of small fibrous masses); score 3, severe (large fibrous areas and severe distortion of lung architecture; "honeycomb lung" could be found). Three random visual fields were selected from a slice, and mean score of the slice was taken. These sections were evaluated by two independent pathologists in a blinded manner.

**2.7. Enzyme-Linked Immunosorbent Assay.** The concentrations of IL-6, IL-10, CTGF, and HYP were measured using ELISA Kit (Boster Biological Engineering Co., Ltd., Wuhan, China), according to the manufacturer's instructions. The optical density (OD) value was determined at 450 nm using ELISA reader (Bio-Tek Instruments Inc., Winooski, VT, USA).

**2.8. Immunohistochemistry Analysis.** We performed routine immunohistochemistry to measure the expression of  $\alpha$ -SMA, TGF- $\beta$ 1, CTGF, NOX-4, NOX-2, COX-2, STAT3, MMP-1, MMP-2, MMP-3, MMP-7, MMP-9, CCL3, and CCR1 in lung tissues. Briefly, sections were incubated with antibodies against  $\alpha$ -SMA (1:1000, ab124964, Abcam, Cambridge, UK), TGF- $\beta$ 1 (1:100, MAB240, R&D system, Minneapolis, USA), CTGF (1:200, ab6992, Abcam, Cambridge, UK), NOX-4 (1:150, ab109225, Abcam, Cambridge, UK), NOX-2 (1:500, ab31092, Abcam, Cambridge, UK), COX-2 (1:100, ab52237, Abcam, Cambridge, UK), STAT3 (1:75, ab76315, Abcam, Cambridge, UK), MMP-1 (1:200, ab137332, Abcam, Cambridge, UK), MMP-2 (1:125, ab37150, Abcam, Cambridge, UK), MMP-3 (1:50, ab52915, Abcam, Cambridge, UK), MMP-7 (1:75, ab5706, Abcam, Cambridge, UK), MMP-9 (1:250, ab76003, Abcam, Cambridge, UK), CCL3 (0029590101, ABclonal, China), and CCR1 (ZP4113BBP13, Boster, China) at 4°C overnight. After washing off the unbound antibodies

with PBS, the sections were incubated with biotinylated anti-rabbit secondary antibody (ZSGB-BIO, Beijing, China) at room temperature for 1 h and then were visualized with diaminobenzidine. Intensity and quantity of stained sections was evaluated using a semiquantitative immunoreactivity score (IRS) [30]. Three random visual fields were selected from a section to score staining intensity (scored as A) and positive cell ratio (scored as B), that is, for A: 0, negative staining; 1, light-yellow staining; 2, pale-brown staining; 3, dark-brown staining. In parallel, for B: 0, no cells stained; 1, fewer than 10% of cells stained; 2, 10% to 50% of cells stained; 3, 51% to 80% of cells stained; 4, more than 81% of cells stained. The average of five fields was the final score of each section (calculated by multiplying A and B).

**2.9. Statistical Analysis.** Data were expressed as mean  $\pm$  SEM. Multiple comparison was assessed by one-way analysis of variance (ANOVA) using SPSS 17.0 software.  $P < 0.05$  was considered to be significant.

### 3. Results

**3.1. CTS Prevented Weight Loss of RILI Rats.** First, we observed the impacts of CTS on the body weight, which serve as an important indicator of the general health condition, in RILI rats. Model RILI rats had notable lower body weight after month 3, as compared to control rats (Figure 1). CTS administration could partly preserve body weight, suggesting the rescuing efficacy of CTS in radiation-induced lung injury.

**3.2. CTS Preserved Pulmonary Function of RILI Rats.** Tidal volume, maximum voluntary ventilation, and respiratory rates were evaluated as crucial indicators in pulmonary function testing. As compared with controls, model RILI rats had marked lower tidal volumes and maximum voluntary ventilation, as well as higher respiratory rates after 3-month radiation, which suggest a decline of pulmonary function seen in RILI rats. CTS treatment was able to partly restore the tidal volume, maximum voluntary ventilation, and respiratory rates (Figure 2). Our observation indicated that CTS intervention could restore the pulmonary function of RILI rats.

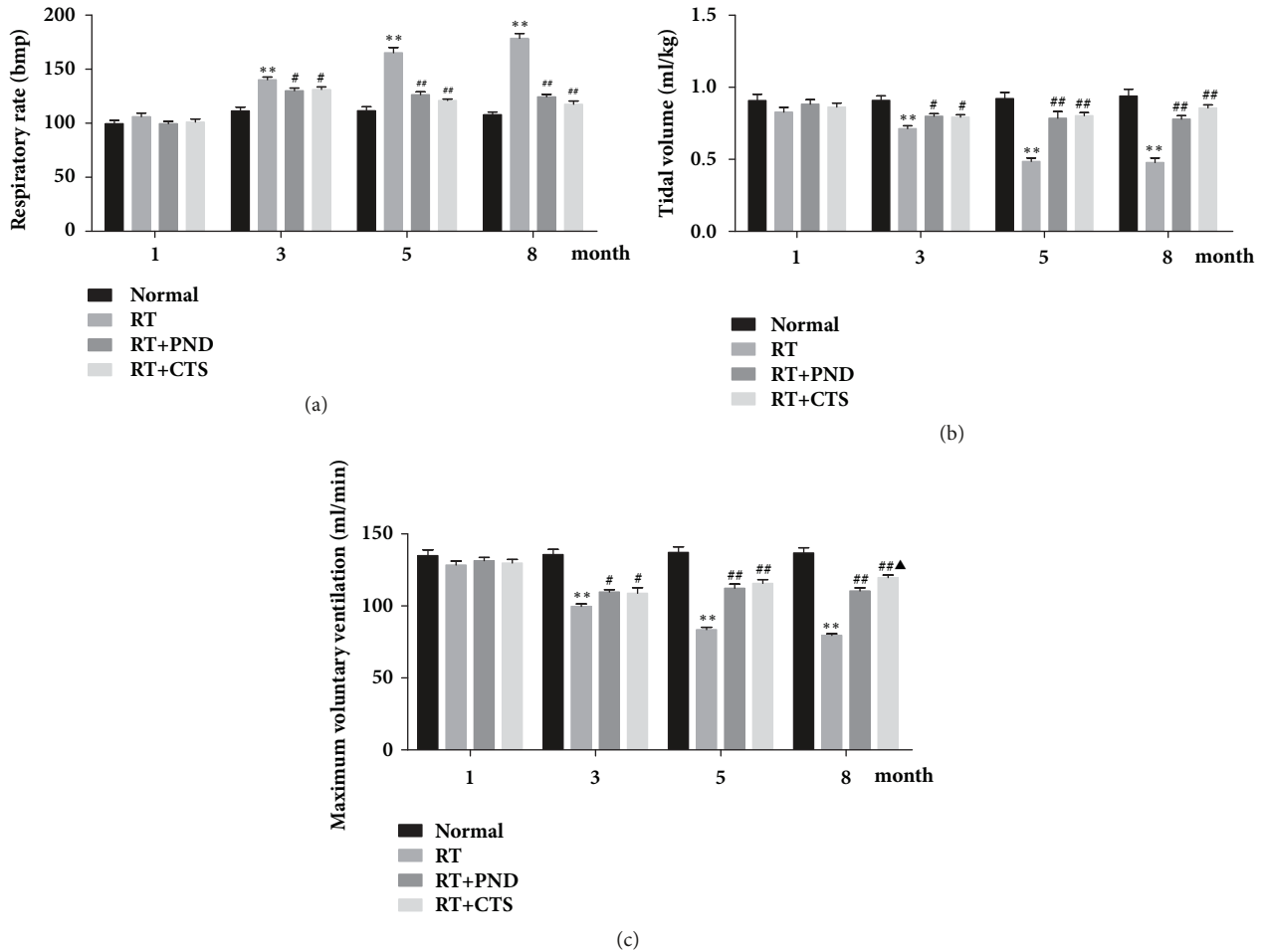


FIGURE 2: Effects of CTS on pulmonary function of RILI rats. (a) Respiratory rates. (b) Tidal volume. (c) Maximum voluntary ventilation.  $n = 6$ . \* $P < 0.05$  and \*\* $P < 0.01$  versus Normal; # $P < 0.05$  and ## $P < 0.01$  versus RT; ▲ $P < 0.05$  and ▲▲ $P < 0.01$  versus RT+PND.

**3.3. CTS Ameliorated RILI Histopathology.** We further examined the pulmonary coefficient and pathological changes in rats from various groups. Pulmonary coefficient is a wet/weight index of lung and reflects the degree of lung inflammation and fibrosis. As displayed in Figure 3(e), pulmonary coefficients were significantly increased in model RILI rats after 1-month radiation. Both CTS and PND treatments potentially restored the pulmonary coefficients of RILI rats.

We also observed the pathological changes in lung tissues on months 1, 3, 5, and 8 by H&E staining; a visible difference between control and model rats was identified in terms of pathological alterations. Lung tissues from model RILI rats presented thickening of the alveolar septa, infiltration of inflammatory cells, and interstitial edema. Moreover, discontinuity in the wall of alveolus was observed after 5-month radiation. Both CTS and PND treatments markedly reduced the radiation-induced morphologic abnormalities (Figures 3(a) and 3(b)). At late phase of RILI, excessive deposition of collagen generally results in progressive loss of pulmonary function. Masson's trichrome staining depicted no noteworthy evidence of pulmonary fibrosis at early stage

of radiation. After 5-month radiation, model RILI rats experienced a robust accumulation of collagenous fibers in thickened alveolar septa and the areas around the bronchiolar. Both CTS and PND treatments significantly attenuated the pulmonary fibrosis, which was reflected by the reduction of collagen sedimentation in lung tissues (Figures 3(c) and 3(d)). Interestingly, CTS exhibited stronger antifibrosis activity than PND treatment, especially after 5-month administration.

**3.4. CTS Reduced  $\alpha$ -SMA and HYP Levels in RILI Rats.**  $\alpha$ -SMA is considered as a specific marker of myofibroblasts, which plays a dominant role in fibrogenesis. Lung tissue immunostaining revealed that  $\alpha$ -SMA levels were gradually and notably elevated with the increment of time after radiation, suggesting that fibrocytes gave rise to increased number of myofibroblasts in injured lung tissue. CTS treatment caused an astonishing reduction of  $\alpha$ -SMA levels in lung tissues, and its inhibitory effect was proved to be significantly stronger than that of PND, especially at month 8 (Figures 4(a) and 4(b)).

HYP is a component of the protein collagen and thus plays a crucial role in collagen stability. We thus assayed HYP



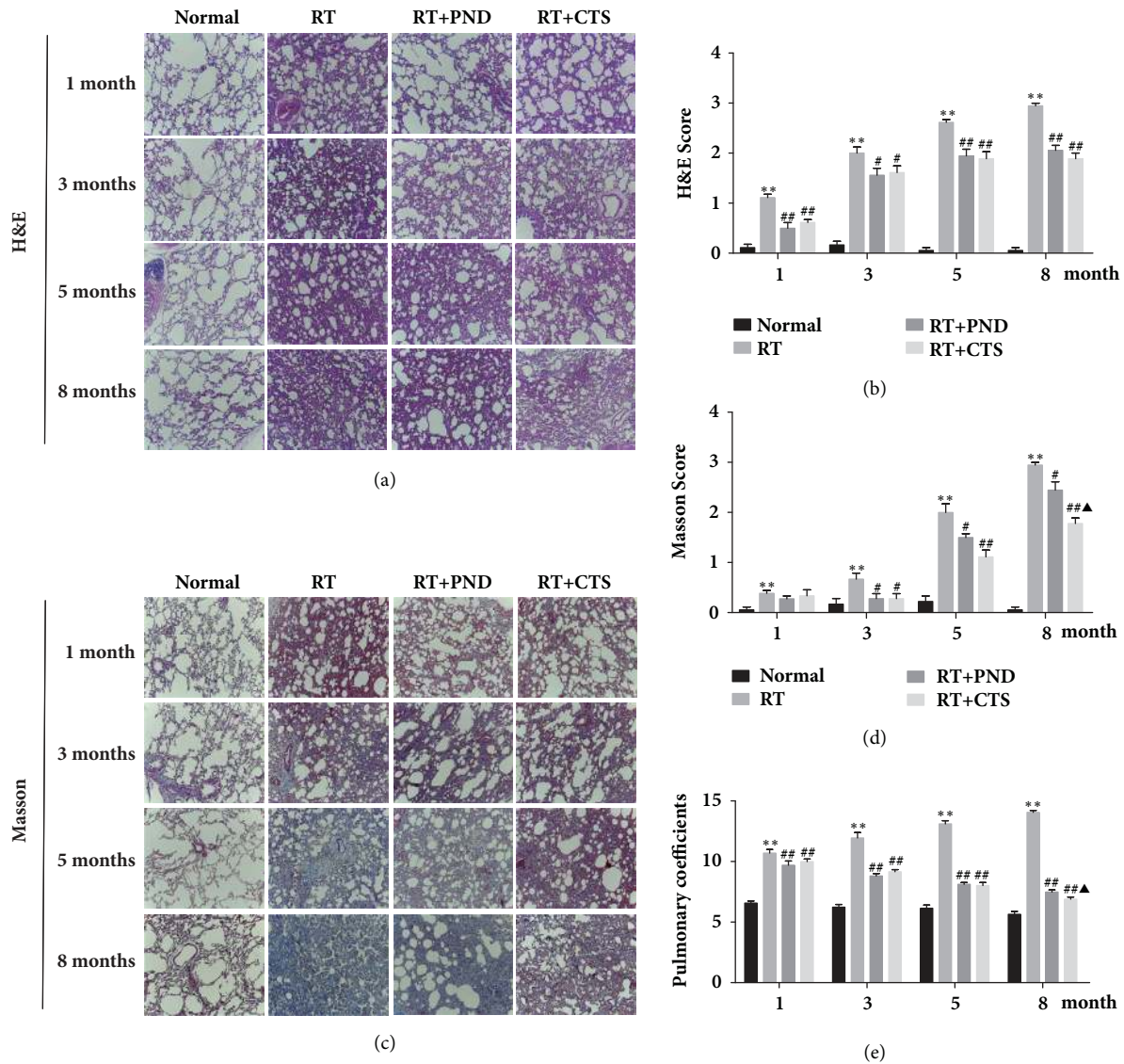


FIGURE 3: CTS ameliorated pulmonary coefficient and histopathology abnormalities in RILI rats. (a) H&E-stained lung tissue in each group (magnification  $\times 20$ ). (b) Semi-quantitative analysis of H & E staining. (c) Masson's trichrome-stained lung tissue in each group (magnification  $\times 20$ ). Blue indicates the collagen deposition. (d) Semi-quantitative analysis of Masson's trichrome staining. (e) Pulmonary coefficient of rats in each group.  $n = 6$ . \*  $P < 0.05$  and \*\*  $P < 0.01$  versus Normal; #  $P < 0.05$  and ##  $P < 0.01$  versus RT; ▲  $P < 0.05$  and ▲▲  $P < 0.01$  versus RT+PND.

levels in lung tissue homogenates. As depicted in Figure 4(c), radiation led to significant increase of HYP content, which could be reversed remarkably by both CTS and PND treatments. These results indicated that CTS could suppress excessive activation of myfibroblasts, thereby reducing the collagen sedimentation and then attenuate radiation-induced pulmonary fibrosis.

**3.5. CTS Decreased TGF- $\beta$ 1 Production in RILI Rats.** To further elucidate the protective effect of CTS against radiation-induced pulmonary fibrosis, we measured the profibrotic cytokines TGF- $\beta$ 1 and CTGF in treated rats. TGF- $\beta$ 1 is a crucial profibrotic cytokine and has a huge role in initiating differentiation of fibroblasts into myfibroblasts and accelerating the synthesis of collagen, as evidenced by a large number

of studies [31]. Lung tissue immunostaining displayed a gradual and significant increase of TGF- $\beta$ 1 expression in model RILI rats at months 1, 3, 5, and 8 after radiation, respectively. CTS and PND treatments could potently suppress TGF- $\beta$ 1 releasing, and we observed a slight stronger inhibition effect of CTS treatment when compared to PND treatment, although it did not achieve statistical significance (Figures 5(a) and 5(b)).

CTGF is a member of the Cyr61-CTGF-Nov protein family, and it is recognized to be implicated in fibroblast proliferation and collagen synthesis. Figure 5(e) clearly showed that CTGF levels were dramatically elevated in plasma samples from RILI rats after month 3. However, there was little antagonistic effect on CTGF offered by CTS administration during the entire radiation period. This result

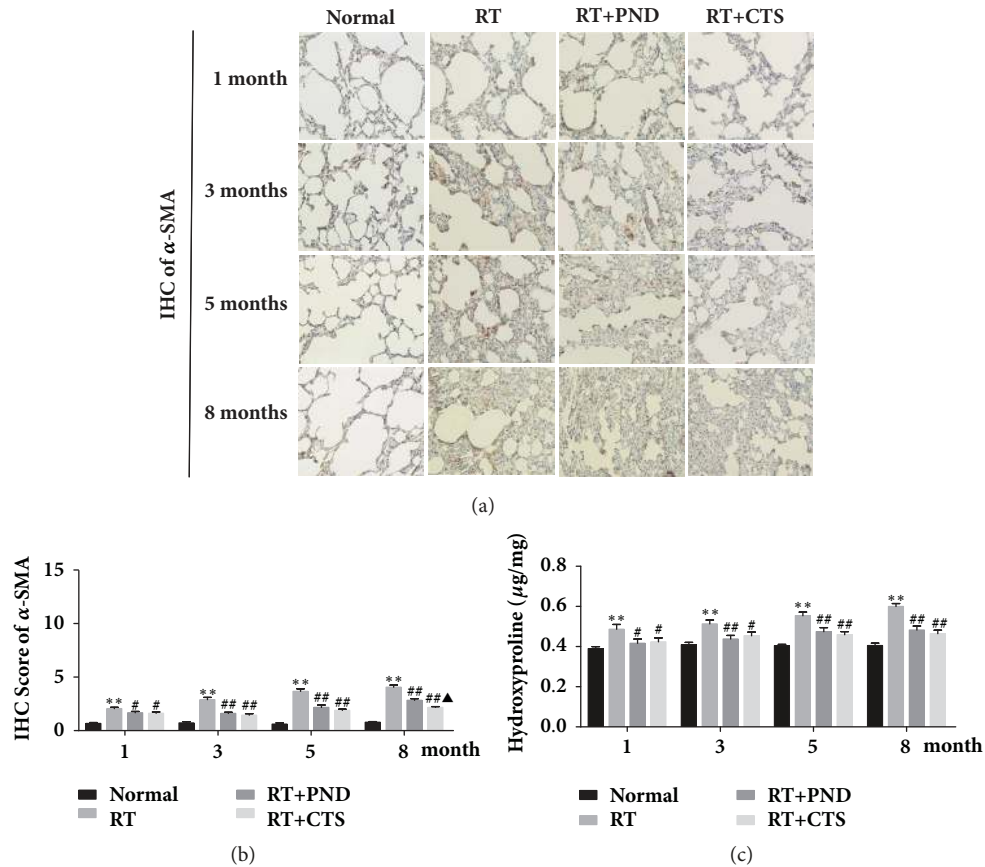


FIGURE 4: CTS reduced  $\alpha$ -SMA and HYP levels in RILI rats. (a) IHC staining of  $\alpha$ -SMA in lung tissue sections from each group (magnification  $\times 200$ ). (b) Semiquantitative analysis of  $\alpha$ -SMA IHC staining. (c) HYP levels of lung homogenates in each group.  $n = 6$ . \* $P < 0.05$  and \*\* $P < 0.01$  versus Normal; # $P < 0.05$  and ## $P < 0.01$  versus RT;  $\blacktriangle P < 0.05$  and  $\blacktriangle\blacktriangle P < 0.01$  versus RT+PND.

was also confirmed by lung tissue immunostaining of CTGF (Figures 5(c) and 5(d)).

**3.6. CTS Inhibited NOX-4 Activation in RILI Rats.** We then evaluate the expressions of NOX-4, NOX-2, STAT3, and COX-2, which were reported to link to TGF- $\beta$ 1 production and fibrogenic responses, in the lung tissues. NOX-4 is an important profibrotic signal implicated in aberrant fibroblast activation in idiopathic pulmonary fibrosis [32], and TGF- $\beta$ 1-mediated collagen type I gene,  $\alpha$ -SMA, and fibronectin-1 gene expressions were Nox4-dependent [33, 34]. Additionally, COX-2 is regarded as an antifibrotic enzyme involved in repressing fibroblast-to-myofibroblast differentiation. Reduced COX-2 expression has been observed in patients with idiopathic pulmonary fibrosis [35], and TGF- $\beta$  stimulation lowered levels of COX-2 and thereby contributing to the activation of lung fibroblasts and excessive collagen deposition in pulmonary fibrosis [36].

In the present study, we demonstrated a striking difference in the range and distribution of NOX-4 and COX-2 between normal and radiated lung tissues. As shown in Figures 6(a) and 6(b), NOX-4 protein levels were mounting sharply after radiation, both PND and CTS treatments obviously attenuated NOX-4 activation in radiated lung tissues.

Also, we noted that CTS suppression was slightly stronger as compared to PND treatment. CTS, however, exhibited little effect on the decreased COX-2 expressions elicited by radiation (Figures 6(c) and 6(d)). Although NOX-2 and STAT3 were partly shown to be implicated in tissue fibrosis, barely the radiated lung tissues present evidence of elevated or reduced NOX-2 and STAT3 expressions (data not shown). Together, CTS could notably attenuate radiation-induced activation of NOX-4 in lung tissues.

**3.7. CTS Significantly Enhanced MMP-1 Levels in RILI Rats.** Fibrosis is pathologically characterized by the excessive matrix accumulation, frequently caused not only by enhanced matrix synthesis, but also by decreased matrix degradation [37]. Matrix metalloproteinases (MMPs) are zinc-dependent endopeptidases that degrade extracellular matrix proteins and thus participate in extracellular matrix remodeling, acting as a powerful brake on the decreased matrix degradation. MMPs superfamily includes multiple types, of which MMP-1 [38, 39], MMP-2 [40], MMP-3 [41], MMP-7 [42], and MMP-9 [40] have been shown to be implicated in the fibrotic process of lung tissues.

To uncover whether CTS affect these enzymes contributing to the degradation of excessive matrix, its effects

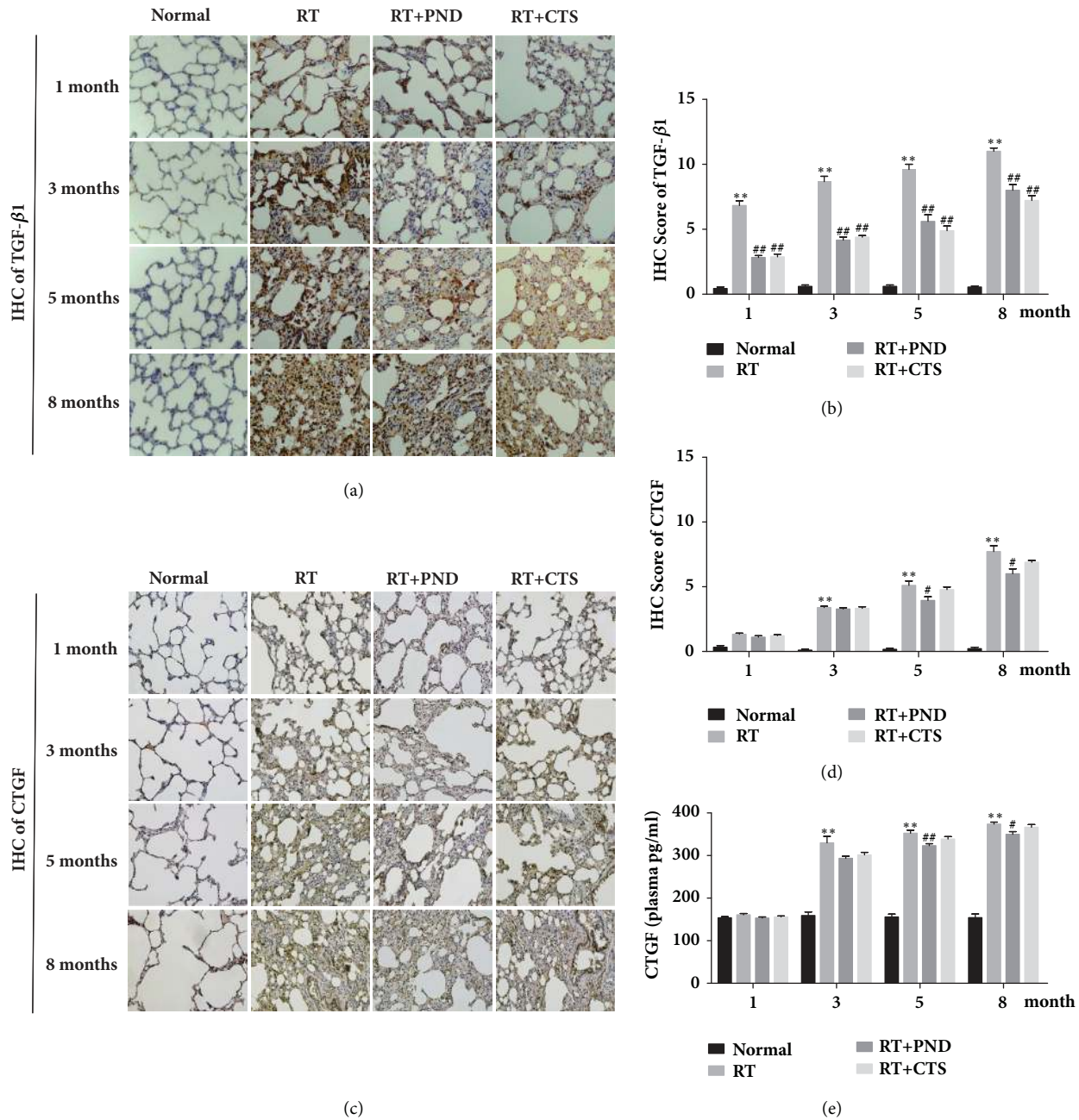


FIGURE 5: Effects of CTS on TGF-β1 and CTGF levels in RILI rats. (a) IHC staining of TGF-β1 in lung tissue sections from each group (magnification × 200). (b) Semi-quantitative analysis of TGF-β1 IHC staining. (c) IHC staining of CTGF in lung tissue sections from each group (magnification × 200). (d) Semi-quantitative analysis of CTGF IHC staining. (e) Plasma CTGF levels in each group. n = 6. \*P < 0.05 and \*\*P < 0.01 versus Normal; #P < 0.05 and ##P < 0.01 versus RT.

on MMP-1, MMP-2, MMP-3, MMP-7, and MMP-9 were addressed. In the current experiment, a robust accumulation of collagenous fibers in thickened alveolar septa, particularly after 5-month radiation, was noted in parallel with notable suppressed MMP-1 expressions, as depicted in Figures 7(a) and 7(b). CTS prominently enhanced MMP-1 secretion and, intriguingly, CTS administration significantly outperformed PND on enhancing the enzyme levels. MMP-2, MMP-3, MMP-7, and MMP-9 were reported to be partly involved in tissue fibrosis, while in our work, we found no noticeable

change of these enzymes after radiation (data not shown). Together, our findings mirrored CTS's relative superiority over PND in holding the fibrotic process in check, largely, at least in part, by enhancing MMP-1 secretion, which would promote and amplify matrix degradation.

**3.8. CTS Reduced IL-6 and IL-10 Levels in RILI Rats.** ILs is an important group of inflammatory cytokines, and the production and release of ILs were considered to play critical roles in RILI pathogenesis. To recognize whether inhibition



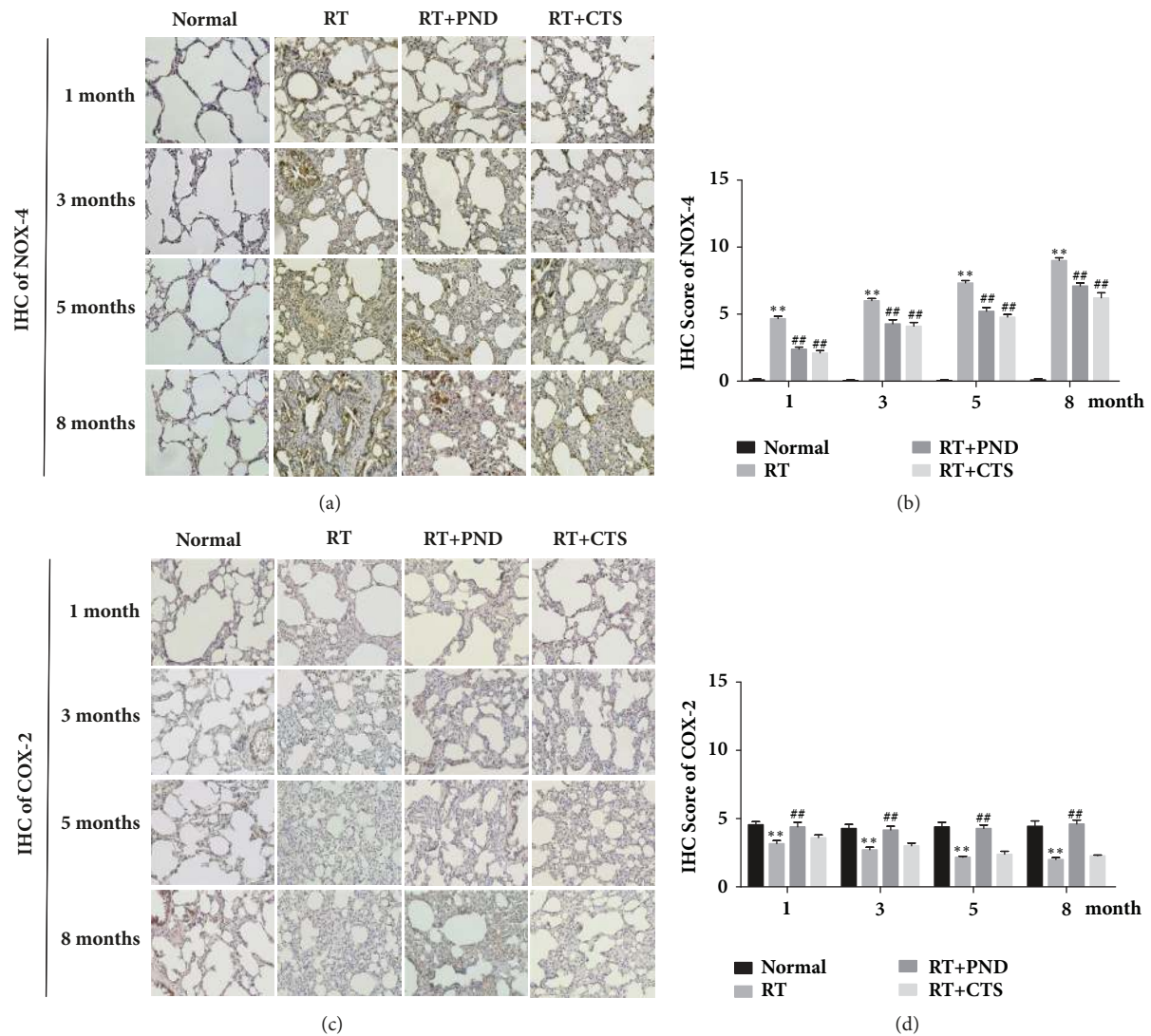


FIGURE 6: Effects of CTS on NOX-4 and COX-2 levels in RILI rats. (a) IHC staining of NOX-4 in lung tissue sections from each group (magnification  $\times 200$ ). (b) Semiquantitative analysis of NOX-4 IHC staining. (c) IHC staining of COX-2 in lung tissue sections from each group (magnification  $\times 200$ ). (d) Semiquantitative analysis of COX-2 IHC staining.  $n = 6$ . \* $P < 0.05$  and \*\* $P < 0.01$  versus Normal; # $P < 0.05$  and ## $P < 0.01$  versus RT.

of CTS on radiation-induced inflammatory response was related to critical inflammatory cytokines IL-6 and IL-10, we sought to assess the concentration of the two cytokine in blood plasma. As shown in Figure 8(a), dramatic increases of plasma IL-6 levels were found after 1-month postradiation. Both CTS and PND treatments produced potent inhibition of IL-6 levels.

Radiation also led to significant increase of IL-10 levels, which is inconsistent with some previous studies [43, 44]. We speculate that a multiple role of cytokine IL-10 in inflammation-associated fibrotic process might be responsible for this result [45]. As shown in Figure 8(b), we found a marked drop of IL-10 levels in CTS-treated rats comparing to model RILI rats. Similar to IL-6, PND had a stronger efficacy than CTS in inhibiting cytokine IL-10. While in this study, we found no notably change of IL-17A in both model and treated

rats (data not shown). Together, CTS act as an inflammatory inhibitor and its anti-inflammatory effect might be attributed to IL-6 and IL-10 inhibition.

**3.9. CTS Inhibited CCL3 and CCR1 Activation in RILI Rats.** Chemokine CCL3 and its receptor CCR1 serve as the key mediators in the dynamic balance of Th1/Th2 in immunocytes, which is crucial in regulating inflammatory and fibrotic responses hooked in RILI process. IHC images depicted that numerous CCL3 and CCR1 positive cells accumulated in the early interstitial inflammation and late fibrosis foci of radiated lung tissues (Figures 9(a) and 9(c)); this finding supports our hypothesis that CCL3/CCR1 activation is implicated in the pathogenic process of RILI.

We also determine whether the accumulation of activated CCL3/CCR1 cells was suppressed in RILI rats after CTS



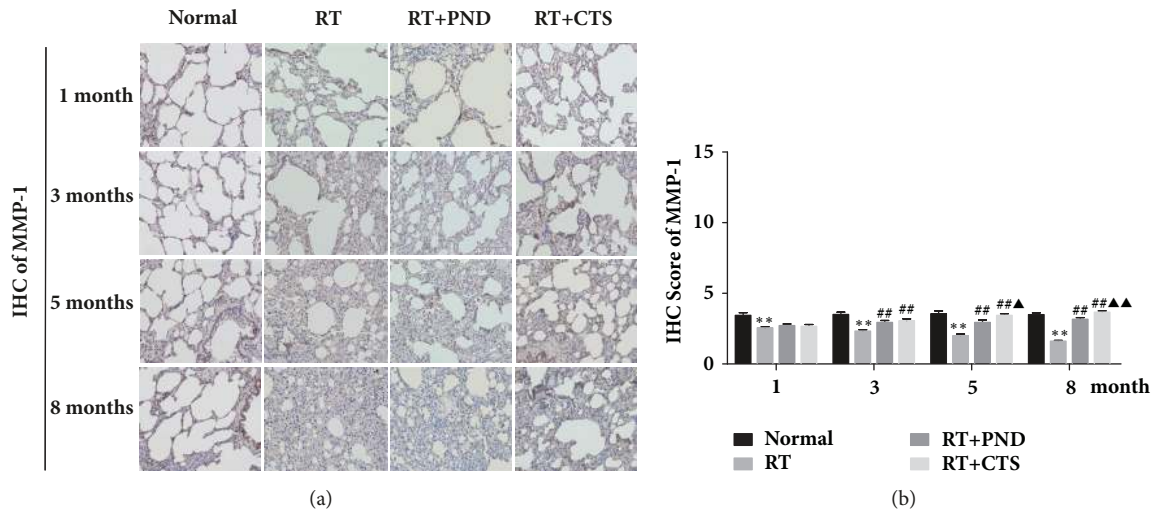


FIGURE 7: Effects of CTS on MMP-1 levels in RILI rats. (a) IHC staining of MMP-1 in lung tissue sections from each group (magnification  $\times$  200). (b) Semi-quantitative analysis of MMP-1 IHC staining.  $n = 6$ . \* $P < 0.05$  and \*\* $P < 0.01$  versus Normal; # $P < 0.05$  and ## $P < 0.01$  versus RT; ▲ $P < 0.05$  and ▲▲ $P < 0.01$  versus RT+PND.

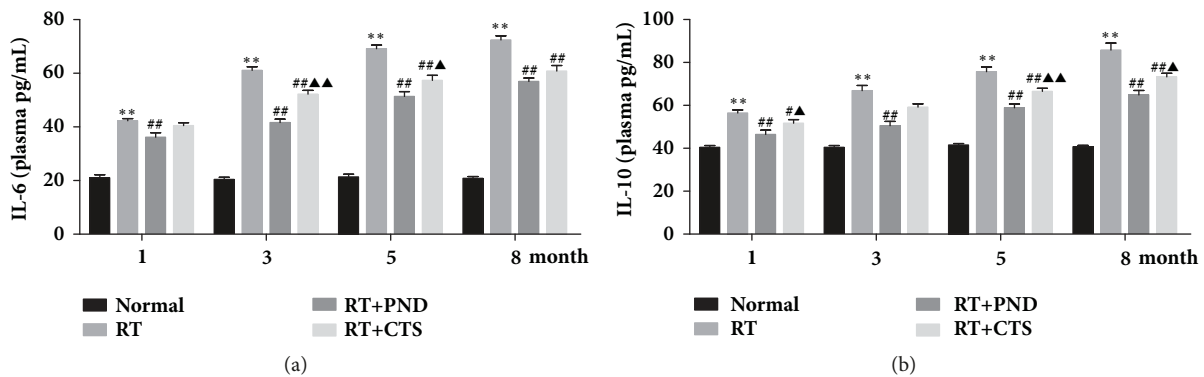


FIGURE 8: CTS reduced IL-6 and IL-10 levels in RILI rats. (a) Plasma IL-6 level in each group. (b) Plasma IL-10 level in each group.  $n = 6$ . \* $P < 0.05$  and \*\* $P < 0.01$  versus Normal; # $P < 0.05$  and ## $P < 0.01$  versus RT; ▲ $P < 0.05$  and ▲▲ $P < 0.01$  versus RT+PND.

administration. CTS and PND produced marked inhibition of CCL3 and CCRI levels in lung tissues of RILI rats, ascertained by immunohistochemistry (Figures 9(a)–9(d)). While CTS led to a clear drop of CCRI levels at month 3 (Figure 9(d)), there was no statistical significance. We speculated that limitation of rat sample size might factor in the nonsignificance. Moreover, in the majority of CTS-treated lung tissues, CCL3/CCRI inhibition was frequently paralleled with the restoration of pathological abnormalities including inflammatory infiltration and collagen sedimentation. Collectively, CTS could ameliorate radiation-induced interstitial inflammation and fibrosis by its mitigating effect on CCL3/CCRI activation.

#### 4. Discussion

RILI is mainly characterized by chronic inflammation and the compensatory fibrosis in lung tissue. Since some clinical adverse effects have been observed with long term therapy

with PND in RILI patients, the pursuit to discover alternative therapies to treat RILI is of high concern. CTS exhibit a board spectrum of anti-inflammatory properties [24, 25] and show important therapeutic activities in cardiac fibrosis [26]. Therefore, CTS might be a promising agent that selected to reduce radiation-induced lung injury.

In early stage, radiation causes inflammatory response and then stimulates burst of inflammatory cytokines, accompanying with macrophages or neutrophils infiltration in lung tissue. In this study, we demonstrated the infiltration of macrophages and neutrophils and interstitial edema, as well as thickening of alveolar septa in radiated lung tissue. Both CTS and PND treatments could reduce the pathological alterations of chronic inflammation in lung tissue, especially the macrophages and neutrophils infiltration. Corroborating with this, CTS and PND treatments also efficiently restored pulmonary coefficient. Since ILs have a huge role in the pathogenesis of lung inflammatory, we next examined the levels of inflammatory cytokines IL-6 and IL-10. IL-6 was a classic proinflammatory cytokine and its plasma levels were

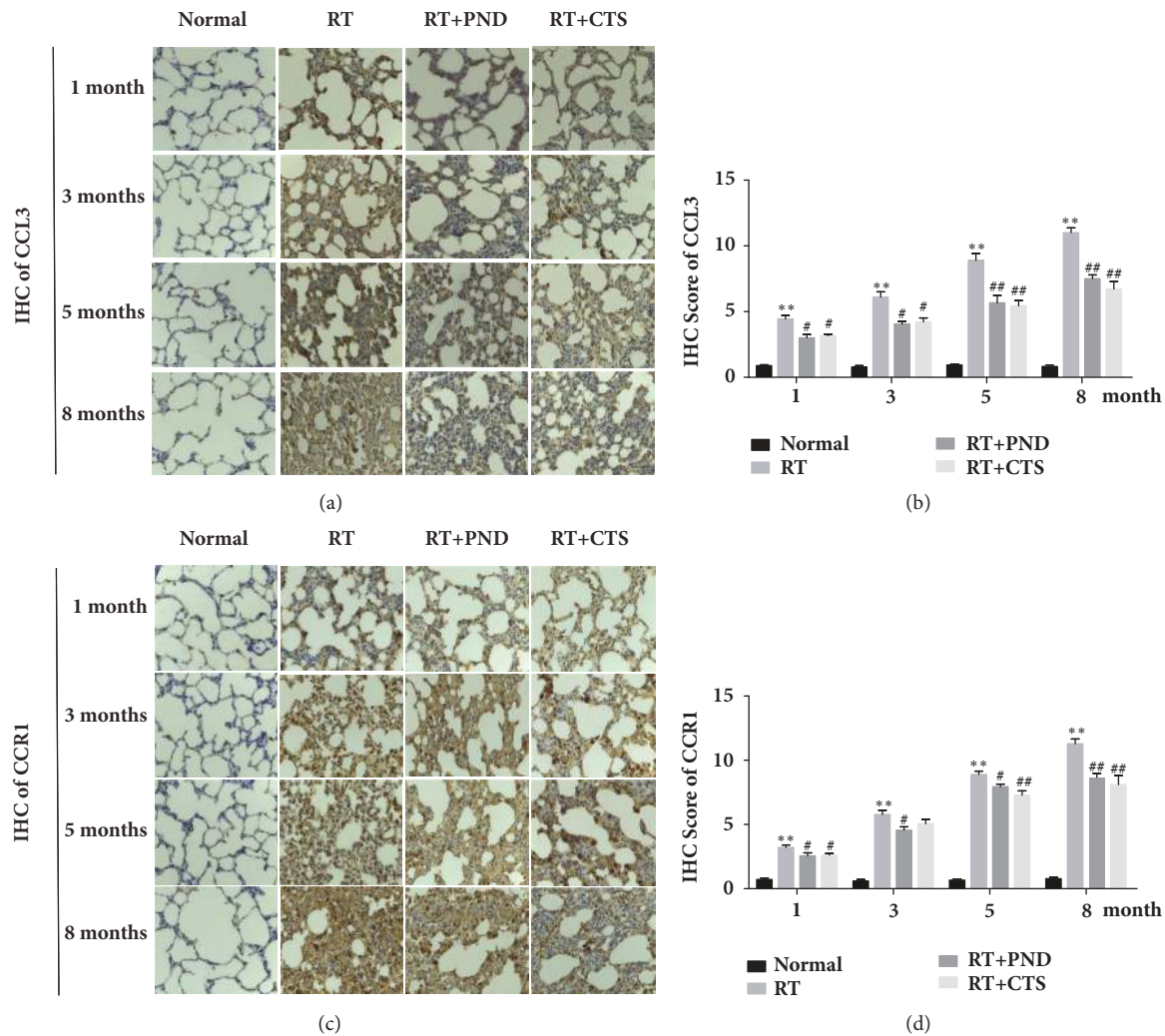


FIGURE 9: CTS inhibited CCL3 and CCR1 activation in RILI rats. (a) IHC staining of CCL3 in lung tissue sections from each group (magnification  $\times 200$ ). (b) Semiquantitative analysis of CCL3 IHC staining. (c) IHC staining of CCR1 in lung tissue sections from each group (magnification  $\times 200$ ). (d) Semiquantitative analysis of CCR1 IHC staining.  $n = 6$ . \* $P < 0.05$  and \*\* $P < 0.01$  versus Normal; # $P < 0.05$  and ## $P < 0.01$  versus RT.

found to increase after radiation in our work. IL-10 is often considered as an anti-inflammatory cytokine, and a couple of works have shown that levels of inflammatory cytokine IL-10 were decreased in rats with radiation-induced lung injury [43, 44]. However, another investigator revealed that the total amount of IL-10 in lung tissue is increased after radiation [45], and lung fibroblasts are able to stimulate the synthesis and release of IL-10 in peripheral blood monocytes [46]; similar results have been observed in our work. IL-10 may play multiple roles in inflammation-associated fibrotic process, since it is an anti-inflammatory cytokine but also a TH2 cytokine with inherent profibrotic effect [45]. Importantly, we found that CTS could inhibit the excessive production and release of IL-6 and IL-10 in RILI rats. PND, by comparison, had a better effect than CTS in ameliorating pulmonary chronic inflammation, as evidenced by pathological examination, pulmonary coefficient, and inflammatory cytokines detection.

In late stage of RILI, pulmonary fibrosis replaced inflammation as the prime concern. We noted that model RILI rats experienced marked fibrotic changes, especially after 5-month radiation. Both CTS and PND alleviated the late stage pulmonary fibrosis to varying degrees. Amazingly, CTS exhibited stronger antifibrosis activity than PND treatment, this result was supported by Masson's trichrome stain as well as by reduced expressions of HYP (fibrosis marker) and  $\alpha$ -SMA (marker of myofibroblast). Thus, comparing to the PND treatment, the advantage of CTS treatment might be its antifibrosis ability rather than its anti-inflammation activity.

We were further interested to probe the protective mechanisms of CTS against radiation-induced pulmonary fibrosis. Fibrogenic process was due, in part, to enhanced matrix synthesis, proposed to be evoked by multiple profibrotic factors, and, in part, to the decreased matrix degradation. We first measured whether CTS influenced the profibrotic

factors CTGF, TGF- $\beta$ 1, STAT3, NOX-4, and NOX-2. TGF- $\beta$ 1 is long considered to as a central mediator facilitating fibrotic process. TGF- $\beta$ 1 stimulation could increase the expression of  $\alpha$ -SMA [47], and thus accelerate HYP deposition. In addition, NOX-4-dependent generation of hydrogen peroxide (H<sub>2</sub>O<sub>2</sub>) is required for TGF- $\beta$ 1-induced myofibroblast differentiation and extracellular matrix production [34]. CTGF serves as another profibrotic signal in tissue remodeling and fibrosis [48], and CTGF blocking was reported to attenuate radiation-induced pulmonary fibrosis [49]. In our work, radiation led to increased levels of the above key profibrotic factors, except for NOX-2 and STAT3, in rats. While effective in reducing the levels of TGF- $\beta$ 1 and NOX-4, CTS exhibited little effect on CTGF levels. One possible explanation is that CTGF might not be the therapeutic target of CTS in RILI rats. These findings suggest that CTS could markedly suppress the NOX-4 and TGF- $\beta$ -induced myofibroblast differentiation, thereby reducing the synthesis of collagen, but act independently of CTGF. Although we noted a slight stronger inhibition effect of CTS treatment when compared to PND in this process, no significant differences were achieved.

We then evaluate whether CTS's antifibrotic bioactivity was partially acquired by regulating antifibrotic molecules COX-2, MMP-1, MMP-2, MMP-3, MMP-7, and MMP-9. MMPs are widely acknowledged to act as a powerful brake on excessive matrix deposition through its essential roles in breaking down components of the extracellular matrix. MMPs thus in particular serve as key antifibrotic molecules in protecting against lung fibrosis. COX-2 is also considered as an antifibrotic enzyme involved in repressing fibroblast-to-myofibroblast differentiation, and there was a feedback relationship between matrix stiffening, COX-2 suppression, and fibroblast activation that promotes and amplifies progressive fibrosis [39]. In this experiment, while barely abrogating the COX-2 suppression elicited by radiation-driven matrix stiffening, CTS could prominently enhance the secretion levels of MMP-1. Consistent with trichrome staining analysis, CTS treatment, by contrast, was evidently superior to PND in enhancing MMP-1 levels. These findings raise the intriguing possibility that CTS has a relative advantage over PND in driving the degradation of excessive matrix evoked by radiation exposure and that MMP-1 might be the potential target responsible for CTS's antifibrotic effectiveness.

CCL3 binding to its receptor CCRI was traditionally emphasized as the central mediators in orchestrating the influx of inflammatory cells into sites of tissue injury [50, 51]. It has recently been reported that a marked increase of CCL3 mRNA expression was observed in inflamed paws, with CCL3 protein detected in neutrophils and macrophages, supporting its involvement in inflammatory responses [52]. The selective interaction of chemokine CCL3 with its receptor, CCRI, is also crucial for thoracic radiation-induced pulmonary fibrosis. Radiated mice develop a marked fibrotic pathology including increased septal thickness and increased collagen deposition, with disturbed lung architecture. By contrast, radiated mice lacking CCL3 or CCRI had no significant septal thickening and small foci of collagen deposition [53], and CCL3/CCRI inhibitor could largely prevent fibrogenic

process. A similar pivotal role of CCRI was found in another bleomycin-induced lung fibrosis mouse model [54]. Besides, a targeted null mutation of CCRI also decreased IL-13-derived inflammation and alveolar remodeling [55]. Another study reported a significant increase in mast cell secretion of key growth factors and cytokines, such as IL-6, TNF- $\alpha$ , and TGF- $\beta$ 1, upon CCRI-FcepsilonRI costimulation [7]. These observations above indicated that CCL3/CCRI axle is crucial for promoting secretion of various inflammatory and fibrotic cytokines. In our work, IHC images depicted that numerous CCL3 and CCRI positive cells accumulated in the early interstitial inflammatory site and late fibrosis foci in radiated lung tissues. Aberrant activation of CCL3/CCRI orchestrated the influx of inflammatory cells to the injured sites and triggered tissue repair mechanisms, thereby exacerbating the insult and driving pulmonary fibrosis. In contrast, RILI rats treated with CTS developed less CCL3 and CCRI positive cells in lung tissues. Collectively, the anti-RILI effect of CTS was possibly achieved by regulating the inflammatory and fibrotic cytokines via inhibiting CCL3/CCRI activation.

Overall, our study on CTS in treating rats with radiation-induced lung injury was encouraging. However, there were also some limitations. For instance, we used only a single dose of CTS, and dose dependence manner of CTS treatment remains unexplored. Besides, the superiority of CTS in antifibrosis ability and its detailed mechanisms merit further investigation in larger sample size studies.

## 5. Conclusion

In summary, CTS could preserve pulmonary function and attenuate radiation-induced lung injury, especially pulmonary fibrosis, in rats. This mitigating effect was partly achieved by suppressing release of inflammatory cytokines IL-6 and IL-10 as well as by balancing levels of fibrotic factors TGF- $\beta$ 1, NOX-4, and MMP-1 and by inhibiting CCL3/CCRI activation. (1) CTS act as an inflammatory inhibitor and its anti-inflammatory effect might be attributed to IL-6 and IL-10 inhibition. (2) In parallel with the reduction of fibrosis, CTS treatment not only effectively diminishes radiation-induced overproduction of profibrotic factors TGF- $\beta$ 1 and NOX-4 but also notably rescues the suppression of antifibrotic proteases MMP-1 secretion.

## Data Availability

The data used to support the findings of this study are available from the corresponding author upon request.

## Conflicts of Interest

The authors declare that they have no conflicts of interest.

## Authors' Contributions

Yifang Jiang and Fengming You contributed equally to the work



## Acknowledgments

This work was funded by the National Natural Science Foundation of China (nos. 81473669, 81774284, and 81804066) and the Project of Science and Technology Department of Sichuan province (nos. 02017RZ005 and 2017SZ0077). We thank Jianxin Xue, Cheng Yi, and He Xu (The West China Hospital of Sichuan University) for their valuable technical advice and assistance.

## Supplementary Materials

(1) Page 1: Weight. Raw data for Figure 1. (2) Page 2-4: Pulmonary Function. Raw data for Figure 2. (3) Page 5-7: H&E and Masson Score, and pulmonary coefficients. Raw data for Figure 3. (4) Page 8-12:  $\alpha$ -SMA and HYP. Raw data for Figure 4. (5) Page 13-18: TGF- $\beta$ 1 and CTGF. Raw data for Figure 5. (6) Page 19-20: NOX-4 and COX-2. Raw data for Figure 6. (7) Page 21: MMP-1. Raw data for Figure 7. (8) Page 22-29: IL-6 and IL-10. Raw data for Figure 8. (9) Page 30-31: CCL3 and CCR1. Raw data for Figure 9. (*Supplementary Materials*)

## References

- [1] L. B. Marks, X. Yu, Z. Vujaskovic, W. Small Jr., R. Folz, and M. S. Anscher, "Radiation-induced lung injury," *Seminars in Radiation Oncology*, vol. 13, no. 3, pp. 333–345, 2003.
- [2] J. E. Meyer, N. K. Finnberg, L. Chen et al., "Tissue TGF- $\beta$  expression following conventional radiotherapy and pulsed low-dose-rate radiation," *Cell Cycle*, vol. 16, no. 12, pp. 1171–1174, 2017.
- [3] P. Zhang, W. Cui, K. G. Hankey et al., "Increased expression of Connective Tissue Growth Factor (CTGF) in multiple organs after exposure of Non-Human Primates (NHP) to lethal doses of radiation," *Health Physics Journal*, vol. 109, no. 5, pp. 374–390, 2015.
- [4] F. Tang, R. Li, J. Xue et al., "Azithromycin attenuates acute radiation-induced lung injury in mice," *Oncology Letters*, vol. 14, no. 5, pp. 5211–5220, 2017.
- [5] H.-Q. Zhang, Y.-F. Yau, K.-Y. Szeto, W.-T. Chan, J. Wong, and M. Li, "Therapeutic effect of Chinese medicine formula DSQRL on experimental pulmonary fibrosis," *Journal of Ethnopharmacology*, vol. 109, no. 3, pp. 543–546, 2007.
- [6] Y. Nakasone, M. Fujimoto, T. Matsushita et al., "Host-derived MCP-1 and MIP-1 $\alpha$  regulate protective anti-tumor immunity to localized and metastatic B16 melanoma," *The American Journal of Pathology*, vol. 180, no. 1, pp. 365–374, 2012.
- [7] N. H. Fifadara, C. C. Aye, S. K. Raghuvanshi, R. M. Richardson, and S. J. Ono, "CCR1 expression and signal transduction by murine BMMC results in secretion of TNF- $\alpha$ , TGF $\beta$ -1 and IL-6," *International Immunology*, vol. 21, no. 8, pp. 991–1001, 2009.
- [8] M. V. Ramos, C. Auvynet, L. Poupel et al., "Chemokine receptor CCR1 disruption limits renal damage in a murine model of hemolytic uremic syndrome," *The American Journal of Pathology*, vol. 180, no. 3, pp. 1040–1048, 2012.
- [9] A.-L. Amati, A. Zakrzewicz, K. Siebers et al., "Chemokines (CCL3, CCL4, and CCL5) inhibit ATP-induced release of IL-1 $\beta$  by monocytic cells," *Mediators of Inflammation*, vol. 2017, Article ID 1434872, p. 10, 2017.
- [10] A. E. Williams, R. J. José, J. S. Brown, and R. C. Chambers, "Enhanced inflammation in aged mice following infection with *Streptococcus pneumoniae* is associated with decreased IL-10 and augmented chemokine production," *American Journal of Physiology-Lung Cellular and Molecular Physiology*, vol. 308, no. 6, pp. L539–L549, 2015.
- [11] D. Scholten, D. Reichart, Y. H. Paik et al., "Migration of fibrocytes in fibrogenic liver injury," *The American Journal of Pathology*, vol. 179, no. 1, pp. 189–198, 2011.
- [12] M. Correa-Costa, T. T. Braga, R. J. Felizardo et al., "Macrophage trafficking as key mediator of adenine-induced kidney injury," *Mediators of Inflammation*, vol. 2014, Article ID 291024, p. 12, 2014.
- [13] Y.-J. Wei, S.-L. Li, and P. Li, "Simultaneous determination of seven active components of Fufang Danshen tablet by high performance liquid chromatography," *Biomedical Chromatography*, vol. 21, no. 1, pp. 1–9, 2007.
- [14] L. Xing, Z. Tan, J. Cheng et al., "Bioavailability and pharmacokinetic comparison of tanshinones between two formulations of *Salvia miltiorrhiza* in healthy volunteers," *Scientific Reports*, vol. 7, no. 1, p. 4709, 2017.
- [15] G. Y. Li, C. Yu, Y. H. Chen, and R. X. Zhang, "Efficacy and safety of oral Tanshinone combined with Minocycline in treatment of moderate to severe Acne Vulgaris," *The Chinese Journal of Dermatovenereology*, vol. 31, no. 2, pp. 235–236, 2017.
- [16] Y. Li, W. Wang, Z. Sun et al., "Study on volatile components of Foliage *Ficus microcarpa*," *China Journal of Chinese Materia Medica*, vol. 33, no. 1, pp. 1898–1899, 2008.
- [17] Y. F. Xu, "Influence of Tanshinone combined with mesalazine on high coagulation state in patients with active ulcerative colitis and clinical effect," *Chinese Journal of Integrated Traditional and Western Medicine on Digestion*, vol. 23, no. 4, pp. 245–249, 2015.
- [18] Z. H. Hu and Y. H. Wu, "Efficacy analysis of entecavir combined with tanshinone capsule in the treatment of chronic hepatitis B with liver fibrosis," *Traditional Chinese and western medicine*, vol. 26, no. 3, pp. 243–246, 2016.
- [19] J. Huang, X. Tang, F. Ye, J. He, and X. Kong, "Clinical therapeutic effects of aspirin in combination with fufang danshen diwan, a traditional chinese medicine formula, on coronary heart disease: a systematic review and meta-analysis," *Cellular Physiology and Biochemistry*, vol. 39, no. 5, pp. 1955–1963, 2016.
- [20] T.-Y. Yang, J. C.-C. Wei, M.-Y. Lee, C. M. B. Chen, and K.-C. Ueng, "A randomized, double-blind, placebo-controlled study to evaluate the efficacy and tolerability of Fufang Danshen (*Salvia miltiorrhiza*) as add-on antihypertensive therapy in Taiwanese patients with uncontrolled hypertension," *Phytotherapy Research*, vol. 26, no. 2, pp. 291–298, 2012.
- [21] Z. Xu, H. Jiang, Y. Zhu et al., "Cryptotanshinone induces ROS-dependent autophagy in multidrug-resistant colon cancer cells," *Chemico-Biological Interactions*, vol. 273, pp. 48–55, 2017.
- [22] L. Lu, S. Zhang, C. Li et al., "Cryptotanshinone inhibits human glioma cell proliferation in vitro and in vivo through SHP-2-dependent inhibition of STAT3 activation," *Cell Death & Disease*, vol. 8, no. 5, p. e2767, 2017.
- [23] H.-J. Jin and C.-G. Li, "Tanshinone IIA and cryptotanshinone prevent mitochondrial dysfunction in hypoxia-induced H9c2 cells: association to mitochondrial ROS, intracellular nitric oxide, and calcium levels," *Evidence-Based Complementary and Alternative Medicine*, vol. 2013, Article ID 610694, p. 11, 2013.

- [24] F. Maione, M. Piccolo, S. De Vita et al., "Down regulation of pro-inflammatory pathways by tanshinone IIA and cryptotanshinone in a non-genetic mouse model of Alzheimer's disease," *Pharmacological Research*, vol. 129, pp. 482–490, 2018.
- [25] S. Ma, D. Zhang, H. Lou, L. Sun, and J. Ji, "Evaluation of the anti-inflammatory activities of tanshinones isolated from *Salvia miltiorrhiza* var. *Alba* roots in THP-1 macrophages," *Journal of Ethnopharmacology*, vol. 188, pp. 193–199, 2016.
- [26] S.-H. Lo, C.-T. Hsu, H.-S. Niu, C.-S. Niu, J.-T. Cheng, and Z.-C. Chen, "Cryptotanshinone inhibits STAT3 signaling to alleviate cardiac fibrosis in Type 1-like diabetic rats," *Phytotherapy Research*, vol. 31, no. 4, pp. 638–646, 2017.
- [27] Y. Ma, H. Li, Z. Yue et al., "Cryptotanshinone attenuates cardiac fibrosis via downregulation of COX-2, NOX-2, and NOX-4," *Journal of Cardiovascular Pharmacology*, vol. 64, no. 1, pp. 28–37, 2014.
- [28] S. Ma, D. Yang, K. Wang, B. Tang, D. Li, and Y. Yang, "Cryptotanshinone attenuates isoprenaline-induced cardiac fibrosis in mice associated with upregulation and activation of matrix metalloproteinase-2," *Molecular Medicine Reports*, vol. 6, no. 1, pp. 145–150, 2012.
- [29] Y. Li, S. Shi, J. Gao et al., "Cryptotanshinone downregulates the profibrotic activities of hypertrophic scar fibroblasts and accelerates wound healing: A potential therapy for the reduction of skin scarring," *Biomedicine & Pharmacotherapy*, vol. 80, pp. 80–86, 2016.
- [30] W. Remmele and H. E. Stegner, "Recommendation for uniform definition of an immunoreactive score (IRS) for immunohistochemical estrogen receptor detection (ER-ICA) in breast cancer tissue," *Der Pathologe*, vol. 8, no. 3, pp. 138–140, 1987.
- [31] K. K. Kim, D. Sheppard, and H. A. Chapman, "TGF-beta1 Signaling and Tissue Fibrosis," *Cold Spring Harbor Perspectives in Biology*, vol. 10, no. 4, Article ID a022293, 2018.
- [32] N. Amara, D. Goven, F. Prost, R. Muloway, B. Crestani, and J. Boczkowski, "NOX4/NADPH oxidase expression is increased in pulmonary fibroblasts from patients with idiopathic pulmonary fibrosis and mediates TGFβ1-induced fibroblast differentiation into myofibroblasts," *Thorax*, vol. 65, no. 8, pp. 733–738, 2010.
- [33] H. Dosoki, A. Stegemann, M. Taha et al., "Targeting of NADPH oxidase in vitro and in vivo suppresses fibroblast activation and experimental skin fibrosis," *Experimental Dermatology*, vol. 26, no. 1, pp. 73–81, 2017.
- [34] L. Hecker, R. Vittal, T. Jones et al., "NADPH oxidase-4 mediates myofibroblast activation and fibrogenic responses to lung injury," *Nature Medicine*, vol. 15, no. 9, pp. 1077–1081, 2009.
- [35] D. K. Petkova, C. A. Clelland, J. E. Ronan, S. Lewis, and A. J. Knox, "Reduced expression of cyclooxygenase (COX) in idiopathic pulmonary fibrosis and sarcoidosis," *Histopathology*, vol. 43, no. 4, pp. 381–386, 2003.
- [36] E. Takai, M. Tsukimoto, and S. Kojima, "TGF-beta1 downregulates COX-2 expression leading to decrease of PGE2 production in human lung cancer A549 cells, which is involved in fibrotic response to TGF-beta1," *PLoS ONE*, vol. 8, no. 10, Article ID e76346, 2013.
- [37] Y. Iimuro and D. A. Brenner, "Matrix metalloproteinase gene delivery for liver fibrosis," *Pharmaceutical Research*, vol. 25, no. 2, pp. 249–258, 2008.
- [38] G.-X. Hu, S.-T. Yao, L.-H. Zeng, Y.-Z. Peng, and J. Zheng, "Effects of hydroxycamptothecin on the expression of matrix metalloproteinase-1 (MMP-1), tissue inhibitor of MMP-1, and type I collagen in rats with pulmonary fibrosis," *Genetics and Molecular Research*, vol. 14, no. 2, pp. 4625–4632, 2015.
- [39] F. Liu, J. D. Mih, B. S. Shea et al., "Feedback amplification of fibrosis through matrix stiffening and COX-2 suppression," *The Journal of Cell Biology*, vol. 190, no. 4, pp. 693–706, 2010.
- [40] S. Chakrabarti and K. D. Patel, "Matrix metalloproteinase-2 (MMP-2) and MMP-9 in pulmonary pathology," *Experimental Lung Research*, vol. 31, no. 6, pp. 599–621, 2005.
- [41] C. M. Yamashita, L. Dolgonos, R. L. Zemans et al., "Matrix metalloproteinase 3 is a mediator of pulmonary fibrosis," *The American Journal of Pathology*, vol. 179, no. 4, pp. 1733–1745, 2011.
- [42] S. Fujishima, T. Shiomi, S. Yamashita et al., "Production and activation of matrix metalloproteinase 7 (matrilysin 1) in the lungs of patients with idiopathic pulmonary fibrosis," *Archives of Pathology & Laboratory Medicine*, vol. 134, no. 8, pp. 1136–1142, 2010.
- [43] X. Jiang, X. Jiang, C. Qu et al., "Intravenous delivery of adipose-derived mesenchymal stromal cells attenuates acute radiation-induced lung injury in rats," *Cytotherapy*, vol. 17, no. 5, pp. 560–570, 2015.
- [44] H. Wang, Y.-F. Yang, L. Zhao et al., "Hepatocyte growth factor gene-modified mesenchymal stem cells reduce radiation-induced lung injury," *Human Gene Therapy*, vol. 24, no. 3, pp. 343–353, 2013.
- [45] M. G. Haase, A. Klawitter, P. Geyer, and G. B. Baretton, "Expression of the immunomodulator IL-10 in type I pneumocytes of the rat: Alterations of IL-10 expression in radiation-induced lung damage," *Journal of Histochemistry & Cytochemistry*, vol. 55, no. 11, pp. 1167–1172, 2007.
- [46] C. Vancheri, C. Mastruzzo, V. Tomaselli et al., "Normal human lung fibroblasts differently modulate interleukin-10 and interleukin-12 production by monocytes: Implications for an altered immune response in pulmonary chronic inflammation," *American Journal of Respiratory Cell and Molecular Biology*, vol. 25, no. 5, pp. 592–599, 2001.
- [47] K.-I. Jeon, R. P. Phipps, P. J. Sime, and K. R. Huxlin, "Antifibrotic actions of peroxisome proliferator-activated receptor gamma ligands in corneal fibroblasts are mediated by beta-catenin-regulated pathways," *The American Journal of Pathology*, vol. 187, no. 8, pp. 1660–1669, 2017.
- [48] W. Zhao, X. Yue, K. Liu et al., "The status of pulmonary fibrosis in systemic sclerosis is associated with IRF5, STAT4, IRAK1, and CTGF polymorphisms," *Rheumatology International*, vol. 37, no. 8, pp. 1303–1310, 2017.
- [49] S. Bickelhaupt, C. Erbel, C. Timke et al., "Effects of CTGF blockade on attenuation and reversal of radiation-induced pulmonary fibrosis," *Journal of the National Cancer Institute*, vol. 109, no. 8, 2017.
- [50] H. Sahin and H. E. Wasmuth, "Chemokines in tissue fibrosis," *Biochimica et Biophysica Acta*, vol. 1832, no. 7, pp. 1041–1048, 2013.
- [51] S. D. Wolpe, G. Davatelis, B. Sherry et al., "Macrophages secrete a novel heparin-binding protein with inflammatory and neutrophil chemokinetic properties," *The Journal of Experimental Medicine*, vol. 167, no. 2, pp. 570–581, 1988.
- [52] M. Llorian-Salvador, S. Gonzalez-Rodriguez, A. Lastra et al., "Involvement of CC chemokine receptor 1 and ccl3 in acute and chronic inflammatory pain in mice," *Basic & clinical pharmacology & toxicology*, vol. 119, no. 1, pp. 32–40, 2016.
- [53] X. Yang, W. Walton, D. N. Cook et al., "The chemokine, CCL3, and its receptor, CCRI, mediate thoracic radiation-induced

pulmonary fibrosis,” *American Journal of Respiratory Cell and Molecular Biology*, vol. 45, no. 1, pp. 127–135, 2011.

- [54] A. Tokuda, M. Itakura, N. Onai, H. Kimura, T. Kuriyama, and K. Matsushima, “Pivotal role of CCR1-positive leukocytes in bleomycin-induced lung fibrosis in mice,” *The Journal of Immunology*, vol. 164, no. 5, pp. 2745–2751, 2000.
- [55] B. Ma, Z. Zhu, R. J. Homer, C. Gerard, R. Strieter, and J. A. Elias, “The C10/CCL6 Chemokine and CCR1 Play Critical Roles in the Pathogenesis of IL-13-Induced Inflammation and Remodeling,” *The Journal of Immunology*, vol. 172, no. 3, pp. 1872–1881, 2004.





**Hindawi**

Submit your manuscripts at  
[www.hindawi.com](http://www.hindawi.com)

